Biomedical Optics EXPRESS

# Quantitative physiology and immunohistochemistry of oral lesions

**Li-Tzu Lee,[1,2,3] Po-Hsiung Chen,[3,4] Chiou-Tuz Chang,[1] John Wang,[5] Yong-Kie Wong,[1,2] and Hsing-Wen Wang[4,6,*]**

[1]*Department of Dentistry, Taichung Veterans General Hospital, Taichung, Taiwan*
[2] *School of Dentistry, National Yang-Ming University,155 Li-Nong Street, Sector 2, Taipei 11221, Taiwan*
[3] *Equal contribution*
[4] *Institute of Biophotonics, National Yang-Ming University,155 Li-Nong Street, Sector 2, Taipei 11221, Taiwan*
[5]*Department of Pathology, Taichung Veterans General Hospital, Taichung, Taiwan*
[6]*Department of Bioengineering, University of Maryland, College Park, MD 20742, USA*
[*]*hwwang@umd.edu*

**Abstract:** Angiogenesis and hypoxia are reported to correlate with tumor aggressiveness. In this study, we investigated the potential of optically measured total hemoglobin concentration (THC) and blood oxygen saturation ($StO_2$) as a quantitative measure of angiogenesis and hypoxia in oral lesions with an immunohistochemical comparison. 12 normal subjects and 40 oral patients (22 oral squamous cell carcinoma (SCC), 18 benign/premalignant lesions including 11 verrucous hyperplasia (VH) and 7 hyperkeratosis/parakeratosis (HK)) were studied. The results showed that the THC measurement was consistent with vascular endothelial growth factor (VEGF) and microvessel staining in the stromal area, but $StO_2$ was not associated with HIF-1α. We observed inflammation induced neovascular formation in the stromal area of VH and HK that were likely attributed to higher-than-control THC and $StO_2$ and resulted in no difference in optical measurements between all lesions. However, we found that in majority of SCC, the ratio of THC and $StO_2$ levels between lesions and the surrounding tissues provide potential distinguishing characteristics from VH, which are not visually differentiable from SCC, with a sensitivity, specificity, and accuracy of 91%, 68%, and 76%, respectively.



**OCIS codes:** (170.1610) Clinical applications; (170.1850) Dentistry; (170.5280) Photon migration; (300.0300) Spectroscopy.

## References and links

1. *GLOBOCAN* (IARC, 2008) Section of Cancer Information. *http://globocan.iarc.fr/factsheets/populations/factsheet.asp?uno=900*
2. B. W. Neville and T. A. Day, "Oral cancer and precancerous lesions," CA Cancer J. Clin. **52**(4), 195–215 (2002).
3. J. J. Sciubba, "Oral cancer. The importance of early diagnosis and treatment," Am. J. Clin. Dermatol. **2**(4), 239–251 (2001).
4. W. H. Binnie and K. V. Rankin, *Oral cancer: clinical and pathologic correlations* (CRC Press, Boca Raton, 1998).
5. M. W. Lingen, J. R. Kalmar, T. Karrison, and P. M. Speight, "Critical evaluation of diagnostic aids for the detection of oral cancer," Oral Oncol. **44**(1), 10–22 (2008).
6. A. Gillenwater, V. Papadimitrakopoulou, and R. Richards-Kortum, "Oral premalignancy: new methods of detection and treatment," Curr. Oncol. Rep. **8**(2), 146–154 (2006).
7. A. Amelink, O. P. Kaspers, H. J. Sterenborg, J. E. van der Wal, J. L. Roodenburg, and M. J. Witjes, "Non-invasive measurement of the morphology and physiology of oral mucosa by use of optical spectroscopy," Oral Oncol. **44**(1), 65–71 (2008).
8. A. Amelink, H. J. Sterenborg, J. L. Roodenburg, and M. J. Witjes, "Non-invasive measurement of the microvascular properties of non-dysplastic and dysplastic oral leukoplakias by use of optical spectroscopy," Oral Oncol. **47**(12), 1165–1170 (2011).
9. R. A. Schwarz, W. Gao, C. Redden Weber, C. Kurachi, J. J. Lee, A. K. El-Naggar, R. Richards-Kortum, and A. M. Gillenwater, "Noninvasive evaluation of oral lesions using depth-sensitive optical spectroscopy," Cancer **115**(8), 1669–1679 (2009).

#195513 - $15.00 USD Received 12 Aug 2013; revised 17 Oct 2013; accepted 22 Oct 2013; published 29 Oct 2013

10. M. G. Müller, T. A. Valdez, I. Georgakoudi, V. Backman, C. Fuentes, S. Kabani, N. Laver, Z. Wang, C. W. Boone, R. R. Dasari, S. M. Shapshay, and M. S. Feld, "Spectroscopic detection and evaluation of morphologic and biochemical changes in early human oral carcinoma," Cancer **97**(7), 1681–1692 (2003).
11. D. C. de Veld, M. Skurichina, M. J. Witjes, R. P. Duin, H. J. Sterenborg, and J. L. Roodenburg, "Autofluorescence and diffuse reflectance spectroscopy for oral oncology," Lasers Surg. Med. **36**(5), 356–364 (2005).
12. N. Subhash, J. R. Mallia, S. S. Thomas, A. Mathews, P. Sebastian, and J. Madhavan, "Oral cancer detection using diffuse reflectance spectral ratio R540/R575 of oxygenated hemoglobin bands," J. Biomed. Opt. **11**(1), 014018 (2006).
13. R. Choe, S. D. Konecky, A. Corlu, K. Lee, T. Durduran, D. R. Busch, S. Pathak, B. J. Czerniecki, J. Tchou, D. L. Fraker, A. Demichele, B. Chance, S. R. Arridge, M. Schweiger, J. P. Culver, M. D. Schnall, M. E. Putt, M. A. Rosen, and A. G. Yodh, "Differentiation of benign and malignant breast tumors by in-vivo three-dimensional parallel-plate diffuse optical tomography," J. Biomed. Opt. **14**(2), 024020 (2009).
14. G. Yu, T. Durduran, G. Lech, C. Zhou, B. Chance, E. R. Mohler 3rd, and A. G. Yodh, "Time-dependent blood flow and oxygenation in human skeletal muscles measured with noninvasive near-infrared diffuse optical spectroscopies," J. Biomed. Opt. **10**(2), 024027 (2005).
15. T. Durduran, G. Yu, M. G. Burnett, J. A. Detre, J. H. Greenberg, J. Wang, C. Zhou, and A. G. Yodh, "Diffuse optical measurement of blood flow, blood oxygenation, and metabolism in a human brain during sensorimotor cortex activation," Opt. Lett. **29**(15), 1766–1768 (2004).
16. V. T. Chang, P. S. Cartwright, S. M. Bean, G. M. Palmer, R. C. Bentley, and N. Ramanujam, "Quantitative physiology of the precancerous cervix in vivo through optical spectroscopy," Neoplasia **11**(4), 325–332 (2009).
17. H. W. Wang, J. K. Jiang, C. H. Lin, J. K. Lin, G. J. Huang, and J. S. Yu, "Diffuse reflectance spectroscopy detects increased hemoglobin concentration and decreased oxygenation during colon carcinogenesis from normal to malignant tumors," Opt. Express **17**(4), 2805–2817 (2009).
18. B. W. Pogue, S. P. Poplack, T. O. McBride, W. A. Wells, K. S. Osterman, U. L. Osterberg, and K. D. Paulsen, "Quantitative hemoglobin tomography with diffuse near-infrared spectroscopy: pilot results in the breast," Radiology **218**(1), 261–266 (2001).
19. H. W. Wang, M. E. Putt, M. J. Emanuele, D. B. Shin, E. Glatstein, A. G. Yodh, and T. M. Busch, "Treatment-induced changes in tumor oxygenation predict photodynamic therapy outcome," Cancer Res. **64**(20), 7553–7561 (2004).
20. H. W. Wang, J. C. Finlay, K. Lee, T. C. Zhu, M. E. Putt, E. Glatstein, C. J. Koch, S. M. Evans, S. M. Hahn, T. M. Busch, and A. G. Yodh, "Quantitative comparison of tissue oxygen and motexafin lutetium uptake by ex vivo and noninvasive in vivo techniques in patients with intraperitoneal carcinomatosis," J. Biomed. Opt. **12**(3), 034023 (2007).
21. H. K. Roy, A. Gomes, V. Turzhitsky, M. J. Goldberg, J. Rogers, S. Ruderman, K. L. Young, A. Kromine, R. E. Brand, M. Jameel, P. Vakil, N. Hasabou, and V. Backman, "Spectroscopic microvascular blood detection from the endoscopically normal colonic mucosa: biomarker for neoplasia risk," Gastroenterology **135**(4), 1069–1078 (2008).
22. C. Mărgăritescu, C. Simionescu, D. Pirici, L. Mogoantă, R. Ciurea, and A. Stepan, "Immunohistochemical characterization of tumoral vessels in oral squamous cell carcinoma," Rom. J. Morphol. Embryol. **49**(4), 447–458 (2008).
23. Z. J. Shang and J. R. Li, "Expression of endothelial nitric oxide synthase and vascular endothelial growth factor in oral squamous cell carcinoma: its correlation with angiogenesis and disease progression," J. Oral Pathol. Med. **34**(3), 134–139 (2005).
24. N. J. Beasley, R. Prevo, S. Banerji, R. D. Leek, J. Moore, P. van Trappen, G. Cox, A. L. Harris, and D. G. Jackson, "Intratumoral lymphangiogenesis and lymph node metastasis in head and neck cancer," Cancer Res. **62**(5), 1315–1320 (2002).
25. R. L. de Cicco, J. C. Watson, D. E. Bassi, S. Litwin, and A. J. Klein-Szanto, "Simultaneous expression of furin and vascular endothelial growth factor in human oral tongue squamous cell carcinoma progression," Clin. Cancer Res. **10**(13), 4480–4488 (2004).
26. Y. K. Wong, C. J. Liu, P. C. Kwan, and S. Y. Chao, "Microvascular density and vascular endothelial growth factor immunoreactivity as predictors of regional lymph node metastasis from betel-associated oral squamous cell carcinoma," J. Oral Maxillofac. Surg. **61**(11), 1257–1262 (2003).
27. M. Gandolfo, A. Keszler, H. Lanfranchi, and M. E. Itoiz, "Increased subepithelial vascularization and VEGF expression reveal potentially malignant changes in human oral mucosa lesions," Oral Surg. Oral Med. Oral Pathol. Oral Radiol. Endod. **111**(4), 486–493 (2011).
28. H. W. Wang, T. C. Zhu, M. E. Putt, M. Solonenko, J. Metz, A. Dimofte, J. Miles, D. L. Fraker, E. Glatstein, S. M. Hahn, and A. G. Yodh, "Broadband reflectance measurements of light penetration, blood oxygenation, hemoglobin concentration, and drug concentration in human intraperitoneal tissues before and after photodynamic therapy," J. Biomed. Opt. **10**(1), 014004 (2005).
29. G. Yu, T. Durduran, C. Zhou, R. Cheng, and A. G. Yodh, "Near-infrared diffuse correlation spectroscopy for assessment of tissue blood flow," in Handbook of Biomedical Optics, D. A. Boas, C. Pitris, and N. Ramanujam, eds. (CRC Press, Boca Raton, 2011), pp. 195–216.
30. S. McGee, J. Mirkovic, V. Mardirossian, A. Elackattu, C. C. Yu, S. Kabani, G. Gallagher, R. Pistey, L. Galindo, K. Badizadegan, Z. Wang, R. Dasari, M. S. Feld, and G. Grillone, "Model-based spectroscopic analysis of the oral cavity: impact of anatomy," J. Biomed. Opt. **13**(6), 064034 (2008).

#195513 - $15.00 USD Received 12 Aug 2013; revised 17 Oct 2013; accepted 22 Oct 2013; published 29 Oct 2013

31. D. J. Rohrbach, N. Rigual, E. Tracy, A. Kowalczewski, K. L. Keymel, M. T. Cooper, W. Mo, H. Baumann, B. W. Henderson, and U. Sunar, "Interlesion differences in the local photodynamic therapy response of oral cavity lesions assessed by diffuse optical spectroscopies," Biomed. Opt. Express **3**(9), 2142–2153 (2012).
32. J. Carlile, K. Harada, R. Baillie, M. Macluskey, D. M. Chisholm, G. R. Ogden, S. L. Schor, and A. M. Schor, "Vascular endothelial growth factor (VEGF) expression in oral tissues: possible relevance to angiogenesis, tumour progression and field cancerisation," J. Oral Pathol. Med. **30**(8), 449–457 (2001).
33. J. A. Nagy, L. F. Brown, D. R. Senger, N. Lanir, L. Van de Water, A. M. Dvorak, and H. F. Dvorak, "Pathogenesis of tumor stroma generation: a critical role for leaky blood vessels and fibrin deposition," Biochim. Biophys. Acta **948**(3), 305–326 (1989).
34. K. J. Davey, S. Perrier, G. Ohe, A. D. Gilbert, A. Bankfalvi, W. P. Saunders, S. L. Schor, and A. M. Schor, "Assessment of vascularity as an index of angiogenesis in periradicular granulomas. Comparison with oral carcinomas and normal tissue counterparts," Int. Endod. J. **41**(11), 987–996 (2008).
35. F. Tanaka, Y. Otake, K. Yanagihara, Y. Kawano, R. Miyahara, M. Li, T. Yamada, N. Hanaoka, K. Inui, and H. Wada, "Evaluation of angiogenesis in non-small cell lung cancer: comparison between anti-CD34 antibody and anti-CD105 antibody," Clin. Cancer Res. **7**(11), 3410–3415 (2001).
36. D. Kademani, J. T. Lewis, D. H. Lamb, D. J. Rallis, and J. R. Harrington, "Angiogenesis and CD34 expression as a predictor of recurrence in oral squamous cell carcinoma," J. Oral Maxillofac. Surg. **67**(9), 1800–1805 (2009).
37. U. K. Zätterström, E. Brun, R. Willén, E. Kjellén, and J. Wennerberg, "Tumor angiogenesis and prognosis in squamous cell carcinoma of the head and neck," Head Neck **17**(4), 312–318 (1995).
38. K. Dellas, M. Bache, S. U. Pigorsch, H. Taubert, M. Kappler, D. Holzapfel, E. Zorn, H. J. Holzhausen, and G. Haensgen, "Prognostic impact of HIF-1 α expression in patients with definitive radiotherapy for cervical cancer," Strahlenther. Onkol. **184**(3), 169–174 (2008).
39. K. Sakata, M. Someya, H. Nagakura, K. Nakata, A. Oouchi, M. Hareyama, and M. Satoh, "A clinical study of hypoxia using endogenous hypoxic markers and polarographic oxygen electrodes," Strahlenther. Onkol. **182**(9), 511–517 (2006).
40. A. Mayer, M. Höckel, and P. Vaupel, "Endogenous hypoxia markers: case not proven!" Adv. Exp. Med. Biol. **614**, 127–136 (2008).
41. N. J. Beasley, R. Leek, M. Alam, H. Turley, G. J. Cox, K. Gatter, P. Millard, S. Fuggle, and A. L. Harris, "Hypoxia-inducible factors HIF-1alpha and HIF-2alpha in head and neck cancer: relationship to tumor biology and treatment outcome in surgically resected patients," Cancer Res. **62**(9), 2493–2497 (2002).

## 1. Introduction

Oral cancer is among the top ten cancers for men in the world and the second most common cancer for men in Southeast Asia [1]. Mortality rates have not improved over the past four decades despite significant advances in treatments [2–4]. It is well recognized that early diagnosis, and thus early treatment, would reduce mortality [5]. Efforts have been made to develop diagnostic aids such as brush cytology, toluidine blue staining, chemiluminescence, and the VELscope (for imaging tissue autofluorescence). These techniques show limited improved diagnostic accuracy compared to the conventional oral examination [5]. While oral examination is the preferred technique for oral cancer screening, it has proven to be difficult even for experienced clinicians [6].

Optical spectroscopy is an attractive option due to its noninvasive nature and relatively low cost. It has been shown in oral lesions to have potential in guided biopsy [7, 8] and aiding diagnosis [9]. Amelink A et al. used differential path-length spectroscopy (DPS) to extract biological information (e.g., blood content, oxygen saturation, and microvascular diameter in mucosal layers) from superficial tissue and show that (1) oral squamous cell carcinoma (SCC) has lower oxygenation and higher blood content compared to normal mucosa [7] and (2) dysplastic lesions exhibited a borderline significant increase in mucosal blood content, but not in oxygen saturation, compared to non-dysplastic lesions [8]. Schwarz RA et al. used diffuse reflectance spectroscopy (DRS) and autofluorescence spectroscopy together to show comparable diagnostic power of early oral cancer screening to that diagnosed by expert physicians [9]. Although DRS in this and other similar studies [10–12] has not provided quantitative biological information, one of the key spectral features chosen for their diagnostic algorithm was increased microvascularization at the upper stromal layer during carcinogenesis.

Other than oral lesions, DRS has been widely shown to provide quantitative physiological information such as total hemoglobin concentration (THC) and tissue blood oxygen saturation ($StO_2$) in the breast [13], muscle [14], brain [15], cervix [16], and colon [17]. DRS-measured THC and $StO_2$ have been well compared and quantified with other methods, and positively

#195513 - $15.00 USD Received 12 Aug 2013; revised 17 Oct 2013; accepted 22 Oct 2013; published 29 Oct 2013

correlate with microvessel density [18] and tissue oxygen level (i.e., hypoxia marker and pO2 electrode probe [19, 20]). Increased THC or blood content has been detected in several studies for the differentiation of benign and malignant or pre-malignant lesions in breast [13] and colon cancer [21], and to differentiate the second grade from normal and the first grade of cervical intraepithelial neoplasia [16]. All of these increases in THC have been attributed to possible stromal angiogenesis.

Angiogenesis plays an important role in tumor growth, invasion, and metastasis [22, 23]. Studies have reported a correlation between vascular density and lymph node metastasis [24]. The vascular endothelial growth factor (VEGF) is one of the angiogenesis-stimulating factors secreted from tumor cells, and has been found to correlate with tumor aggressiveness and lymph node metastasis. It has also been identified as a prognostic indicator [25]. However, controversial data are available as well, on the relationship between angiogenesis and tumor malignancy, metastasis, and prognosis, and on the correlation between VEGF expression and vascular density [26, 27]. These discrepancies could be attributed to the use of a method that only partially reflected the result of angiogenesis. VEGF is still a common biomarker used for measuring angiogenesis and malignancy.

Taken together, a correlation between optical spectroscopy (either DRS or DPS) measured blood content and angiogenesis marker expression (e.g., VEGF expression) in oral lesions would be expected to aid in oral cancer screening by noninvasively accessing angiogenesis. However, such a correlation has not yet been demonstrated in clinical settings. In Taiwan, the three most common oral lesions are hyperkeratosis/parakeratosis (HK, appearing as a white plaque, histologically categorized as benign or premalignant lesion), verrucous hyperplasia (VH, histologically categorized as benign or premalignant lesion), and squamous cell carcinoma (SCC). HK and VH are generally benign but 1-5% are premalignant, with a risk of progression to SCC. HK appears white and is characterized by an additional keratin layer above the epithelial layer of oral mucosa. Importantly, VH and SCC are not visually differentiable. In current routine screening, physicians use differences in color of the lesion as one "pre-screening" method (e.g., to "detect" HK based on its white appearance) and both benign and malignant lesions require biopsy for a definite diagnosis by histological confirmation. Only after the biopsy is completed, a process which takes several weeks, can an appropriate therapy be selected. Therefore, a supplementary methodology to detect oral cancer in real-time with high sensitivity may help start the treatment plan earlier.

In this study, we aimed to examine the relationship between DRS measured THC and angiogenesis, as well as between DRS measured $StO_2$ and hypoxia. We also investigated the possibility of DRS measured-THC and $StO_2$ in aiding the differentiation of these three categories of oral lesions. We performed DRS measurements in SCC, VH, and HK lesions and their surrounding tissues to provide their quantitative physiological information (i.e., THC and $StO_2$), and then biopsied lesion specimens close to one of the sites where DRS measurements were performed for each patient. The excised lesion specimens were stained with immunohistochemistry (IHC) including angiogenesis marker VEGF, vascular markers CD31, CD34, and vWF, and hypoxia marker HIF1α. Here we used four different angiogenic markers instead of a single one to avoid questions due to the staining methods used. Finally, we compared DRS and IHC results.

## 2. Materials and methods

### *2.1 Patient information and optical measurement protocols*

A total of 49 patients were enrolled in this study, conducted at the Department of Oral and Maxillofacial Surgery, Taichung Veterans General Hospital, Taiwan, between 2009 and 2010. The number of patients for each category of lesions, the number of patients who received DRS measurements and/or biopsy for IHC, and patient gender and age information are summarized in Table 1. 5 and 4 patients out of 27 SCC and 11 HK patients, respectively, were lack of calibration data for DRS analysis and thus the number of patients with DRS measurements in these two categories is less than that of patients with IHC in Table 1. The

#195513 - $15.00 USD Received 12 Aug 2013; revised 17 Oct 2013; accepted 22 Oct 2013; published 29 Oct 2013

anatomic sites of 22 SCC lesions include 10 buccal mucosa (BM), 5 tongues, 1 soft-palate/gingival, and 6 unknown (no record). For 11 VH lesions, 5 are in BM, 2 are in tongue, 1 is in gingiva, and 3 are unknown (no record). For 7 HK lesions, 4 are in BM, 2 are in tongue, and 1 is in palate. All patients signed a study-specific informed consent form. All experimental procedures were approved by the Institutional Review Board of Taichung Veterans General Hospital.

DRS measurements were performed through an optical fiber probe which was brought into contact with tissue surface. For each patient, DRS measurements were taken at 3 different locations ("top", "middle", and "bottom" parts) of the lesion site (i.e., SCC, VH, or HK lesion) and at one adjacent tissue site, which is approximately 1cm from the lesion boundary (determined by a single oral surgeon, Lee, L-T) and appeared to be normal according to an experienced oral surgeon (Lee, L-T). Two replicated DRS measurements were performed on each site or location. A total of 6 or 2 measurements were averaged to represent results of the lesion site or adjacent tissue site, respectively. We originally acquired DRS measurements on the adjacent tissue sites (without biopsy) as "normal" sites. However, we found their quantitative physiological information was often similar to that of the lesions sites. We thus acquired additional DRS measurements on normal subjects for the controls. We considered those "adjacent tissue" site measurements as "adjacent tissue" sites instead of "normal" sites. A total of 12 normal subjects who did not exhibit any oral neoplasia or inflammation were measured on their buccal mucosa. In each normal subject, DRS measurements were performed at 10 different locations/sites randomly. The results of these 10 measurements were averaged to represent the value of each normal subject. The data acquisition time of each DRS measurement was between 100 to 300 ms, to maximize the intensity of collected reflectance signals without saturating the detector. Upon completion of the DRS measurements, the lesion tissue specimens were collected at sites close to one of three DRS measurement sites for the routine pathology examination and additional immunohistochemistry. The optical probe was disinfected before and after each patient's DRS measurements with Cidex OPA (Advanced Sterilization Products, Johnson & Johnson Gateway, LLC). Student's t test (2-tailed) was used to compute all p values in this study.

### *2.2 Diffuse reflectance spectroscopy (DRS) instrumentation and analysis*

A continuous wave broadband diffuse reflectance spectroscopy was used to measure tissue optical (i.e., scattering and absorption coefficients) and physiological properties (e.g., THC and $StO_2$), as in our previous study of colon tissues [17]. In brief, the system consisted of a 100 W quartz tungsten halogen lamp (Olympus, Japan), a hand-held surface contact fiber-optic probe (Fiberoptic Systems Inc., Simi Valley, California), a spectrograph (SP-2156, Princeton Instruments-Acton, Acton, Massachusetts), and a −70°C thermoelectrically cooled CCD camera (PIXIS:400BR, Princeton Instruments Inc., Trenton, New Jersey). The fiber-optic probe consisted of a single source and 4 detection fibers (each with a core diameter of 200 μm). These fibers were packed together inside a Teflon tube with an outer diameter approximately 1.6 mm and side-by-side with source-detector separations ρ at 0.6, 1.5, 2.5, and 4 mm, as shown in Fig. 1(A). Each fiber tip was cut to 45° and polished to turn the delivered or collected light at 90°. Special care is needed when applying DRS to measure tissue surface with ρ at this range. In our previous study, we confirmed that the results using diffusion model (P1 approximation) were as good as P3 approximation for ρ at this range. Diffusion model (P1 approximation) was used for fitting in this study. The results reported in this study were analyzed from reflectance spectra at ρ equal to 0.6 and 1.5 mm, in order to limit the collected diffuse light from the epithelial and upper stromal layer of oral tissue.

To fit the data, we computed normalized reflectance spectra, defined as the spectra normalized to the spectrum at ρ equal to 0.6 mm, and then fitted the calculated reflectance spectra to measured reflectance spectra by employing the analytical solution of the diffusion equation with semi-infinite boundary conditions. The wavelength range used for the fitting was between 600 and 800 nm as previous published studies [17, 20, 28]. The detected tissue depth was approximately 1/3 to 1/2 of the source-detection separations (i.e., 0.6 and 1.5 mm)

#195513 - $15.00 USD Received 12 Aug 2013; revised 17 Oct 2013; accepted 22 Oct 2013; published 29 Oct 2013

based on based on our and other published studies [17, 29], and thus was approximately 0.2 to 0.75 mm below the tissue surface. Finally, a nonlinearly constrained optimization function, FMINCON implemented in MATLAB (The MathWorks, Inc., Natick, Massachusetts), was used to globally fit the data to extracts tissue scattering parameters and chromophore concentrations of oxyhemoglobin ($c_{HbO2}$) and deoxyhemoglobin ($c_{Hb}$). THC and $StO_2$ were calculated from these quantities (e.g. THC = $c_{HbO2}$ + $c_{Hb}$, $StO_2$ = $c_{HbO2}$/THC). Representative normalized DRS spectra and fit results from a normal subject and a SCC patient are shown in Figs. 1(B) and 1(D) using 2 separations (ρ = 0.6 and 1.5 mm) and in Figs. 1(C) and 1(E) using 4 separations (ρ = 0.6, 1.5, 2.5, and 4 mm). Four separations were used here, but not used for the rest of the results, to show how well the fit was using 2 or 4 separations. As shown in the figure, the measured DRS spectra fitted very well with calculated results from a homogeneous diffusion model. The extracted (THC, $StO_2$) values are (84 μM, 89%) using 2 separations and (87 μM, 82%) using 4 separations for the normal subject, and are (97 μM, 35%) using 2 separations and (90 μM, 63%) using 4 separations for the SCC patient. However, the extracted THC and $StO_2$ values using 2 or 4 separations could be quite different (not shown here) because tissue heterogeneity is expected at some locations.

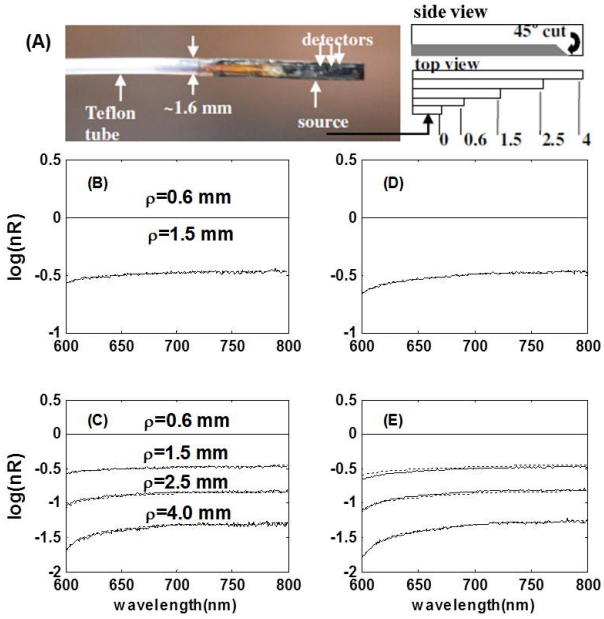


Fig. 1. (A) The photograph and schematic diagram of the fiber optic probe. (B) to (D) show representative measured normalized DRS spectra nR (——) and fitted results (-----) from a normal subject (B, C) and a squamous cell carcinoma (SCC) patient (D, E). The spectra are plotted for two separations (ρ) (B, D) and four separations (C, E). See text for more details on extracted physiological properties.

### *2.3 Immunohistochemistry (IHC)*

The tissue sections were prepared from the incisional biopsy or surgical excision of the lesions. Tissue from oral lesions with pathological diagnosis of hyperkeratosis (HK), verrucous hyperplasia (VH), and oral squamous cell carcinoma (SCC) were stained by hematoxylin and eosin stain (H&E). The LSAB method of IHC was used and tissue processed as follows: cut test sections on Super Frost Plus slides at 3μm, placed the test section at the bottom of the slide, put relevant tissue positive control sections (hepatocellular carcinoma, HCC) on the same slide as the test sections, and put the control section at the frosted end of the slide, being careful not to overlap the patient tissue sections. Reagent negative control with PBS was used as a substitute for the primary antibody. Sections stained by omitting the

#195513 - $15.00 USD Received 12 Aug 2013; revised 17 Oct 2013; accepted 22 Oct 2013; published 29 Oct 2013

primary antibodies were used as negative controls. Slides were dried, de-waxed, rehydrated, washed, quenched, and rinsed subsequently. Endogenous biotin and other non-specific binding with Chemicon blocking solution were blocked for 5 minutes. Then 100μl of primary antibody (mouse monoclonal HIF-1α, 1/200 dilution NeoMarkers, UK) was pipetted onto slide and incubated overnight. Slides were washed with phosphate-buffered saline (PBS) in 5 changes of rinse buffer for 30 seconds. Biotinylated secondary antibody and then streptavidin were applied to slides for 10 minutes each. Finally, any 3,3′-diaminobenzidine (DAB, chromogen) was tipped off onto paper towel and counter-stained in haematoxylin for 20 seconds.

Other immunohistochemical markers were tested: VEGF(AR 483, ready to use BioGenex), CD31(JC/70A, 1/50 dilution, DAKO), CD34(QBEnd10, DAKO), and vWF(MO616, DAKO). In all blood vessel stained micrographs (i.e., vWF, CD31, and CD34 stains), any single brown-stained cell or cluster of endothelial cells that was clearly separated from tumor cells and other connective tissue elements was considered a vessel. The IHC results were reviewed and graded semi-quantitatively by a pathologist (John Wang) and an oral pathologist (LT Lee), using a double-headed light microscope. Grading was assigned to 3 levels: +++ represents overall or more than half of interested area showing positive expression; ++ represents approximately 30 to 50% of interested area showing positive expression; + represents no or little positive expression.

**Table 1. Summary of patient number and the corresponding IHC and DRS measurement results. THC, $StO_2$, rTHC and $rStO_2$ results are expressed as mean ± standard error**

| | | | *SCC* | *Verrucous Hyperplasia (VH)* | Hyperkeratosis/Parakeratosis (HK) |
|---|---|---|---|---|---|
| lesion | IHC | $n_{patient}$ | 27[a] | 11[a] | 11[a] |
| | | $VEGF_{epithelium}$ | ++[b,c] | +++[b] | +++[b] |
| | | $VEGF_{stroma}$ | +++[b] | +++[b] | +++[b] |
| | | $(vWF, CD31, CD34)_{epithelium}$ | +[b,c] | + to ++[b] | + to ++[b] |
| | | $(vWF, CD31, CD34)_{stroma}$ | ++[b] | +++ [b] | +++ [b] |
| | | HIF-1α | ++[b] | ++[b] | ++[b] |
| | DRS | $n_{patient}$, $n_{site}$ | 22, 66 | 11, 33 | 7, 21 |
| | | THC (μM) | 179.7 ± 15.5 | 194.5 ± 27.4 | 195.5 ± 36.5 |
| | | $StO_2$ (%) | 93.1 ± 2.3 | 98.6 ± 0.8 | 91.2 ± 3.3 |
| adjacent | DRS | $n_{patient}$, $n_{site}$ | 22, 22 | 11, 11 | 7, 7 |
| | | THC (μM) | 154.1 ± 16.0 | 182.1 ± 14.7 | 132.7 ± 26.3 |
| | | $StO_2$ (%) | 98.0 ± 0.7 | 95.1 ± 11.3 | 91.7 ± 7.9 |
| lesion/adjacent | DRS | rTHC | 1.42 ± 0.18 | 1.08 ± 0.13 | 1.57 ± 0.26 |
| | | $rStO_2$ | 0.95 ± 0.03 | 1.05 ± 0.05 | 1.09 ± 0.19 |

[a] A total of 49 patients included 43 males and 6 females with ages ranging from 28 to 88 years and an average age of 56 years.
[b] IHC was graded to be +++ (overall or greater than half area having positive expression), ++ (20-50% of area having positive expression), and + (no or little expression).
[c] Tumor cell area, instead of epithelial layers, were graded.

#195513 - $15.00 USD Received 12 Aug 2013; revised 17 Oct 2013; accepted 22 Oct 2013; published 29 Oct 2013

## 3. Results

### *3.1 DRS detected higher total hemoglobin concentration in SCC, VH, and HK lesions, and the adjacent tissues of VH lesions than in the controls*

Because angiogenesis is a key feature of tumorigenesis, we expected to see higher THC in SCC lesions than in VH and HK lesions, the adjacent tissues of SCC, and normal subjects. Figures 2(A) and 2(B) compare the average THC values ( ± standard error) from the buccal mucosa of normal subjects (i.e., the controls) and from the lesion sites and adjacent tissue sites of SCC, VH, and HK patients. The lesion THC from all patients and the adjacent tissue THC of VH lesions are significantly higher (p-value < 0.05) than that from the controls. Figure 2(C) depicts the THC distribution in controls and in all patients. Each data point represents the average THC value for each subject from either the lesion ($n_{site}$ = 3) or the adjacent tissue ($n_{site}$ = 1) of the lesion, or from the buccal mucosa ($n_{site}$ = 10) of a normal subject. All lesions showed much larger THC distribution than the controls. But there was no difference in THC between SCC, VH, and HK lesions.

We calculated the ratio (rTHC) of THC in the lesion over the adjacent tissue for each patient. The results are depicted in Fig. 2(D). The average rTHC values, as well as average THC values, are listed in Table 1. We observed that the adjacent tissues of VH lesions had similar THC to the lesions with a narrower rTHC distribution compared to SCC. SCC patients showed a much broader rTHC distribution with higher rTHC values (e.g., rTHC ≥ 2) in several patients, suggesting the possible angiogenesis detected.

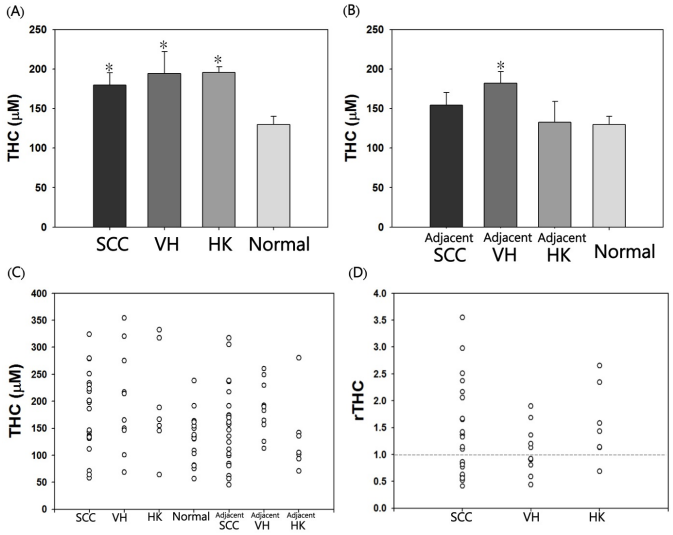


Fig. 2. Bar plots of average total hemoglobin concentration (THC) in lesion (A) and adjacent (B) tissue sites for squamous cell carcinoma (SCC), verrucous hyperplasia (VH), and hyperkeratosis/parakeratosis (HK) patients. Symbol * indicates the average THC value is significantly different from the value of normal subjects, with a p-value less than 0.05. The distribution of THC (C) and the THC ratio (rTHC) (D) for all patients. Each data point represents a single patient.

### *3.2 Immunohistochemistry explains high THC detected in VH and HK lesions was in part due to inflammation*

All patients received IHC. The IHC results are very similar between SCC, VH, or HK lesions. Figures 3 and 4 show the representative H&E and IHC (i.e., VEGF, vWF, CD31, and CD34) micrographs of VH and SCC lesions, respectively. HK had similar IHC results to VH, and their H&E and IHC micrographs are not shown here. Overall, VEGF was stained positive everywhere. In Fig. 3, positive VEGF expression was found in both epithelial and stromal

#195513 - $15.00 USD Received 12 Aug 2013; revised 17 Oct 2013; accepted 22 Oct 2013; published 29 Oct 2013

layers. Unlike VEGF, much higher expressions of vWF, CD31, and CD34 were detected in the stromal layer than in the epithelial layer. These increased blood vessels in the stromal layer were due to inflammatory response induced neovascular formation that often appeared in granulomatous tissues. In SCC patients, we found VEGF expression was mainly localized in the cytoplasm of the tumor cells. As shown in Fig. 4, the tumor nest showed slightly less VEGF expression than surrounding stromal tissues. Peripheral tumoral microvessels or neovascular areas were highlighted by vWF, CD31, and CD34 expressions. Compared to those formed in granulomatous tissues shown in Fig. 3, neovascular areas in SCC were most frequently seen at the margins of the tumor nest with decreased vessel volume. The result of IHC in HIF-1α overall was similar to that of VEGF with a uniform positive expression in all places (data not shown). An average semi-quantitative grading based on the volume of positive expression over all IHC slides is summarized in Table 1. The inflammatory response induced neovascular formation in the stromal layer of VH and HK lesions was in part attributed to the high THC values detected in these lesions (Fig. 2 and Table 1).

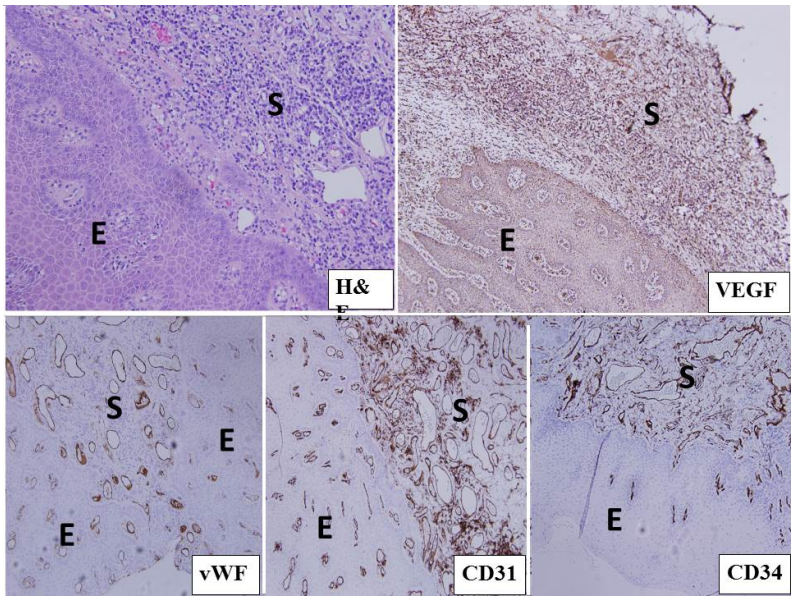


Fig. 3. H&E and immunohistochemical staining, including VEGF, vWF, CD31, and CD34 of verrucous hyperplasia tissue specimens. Endothelial cell-lined blood vessels were stained positive for VEGF, vWF, CD31, and CD34, especially in the granulomatous tissue in the stromal tissue layer. Symbols E and S represent epithelial and stromal layer, respectively.

#195513 - $15.00 USD Received 12 Aug 2013; revised 17 Oct 2013; accepted 22 Oct 2013; published 29 Oct 2013

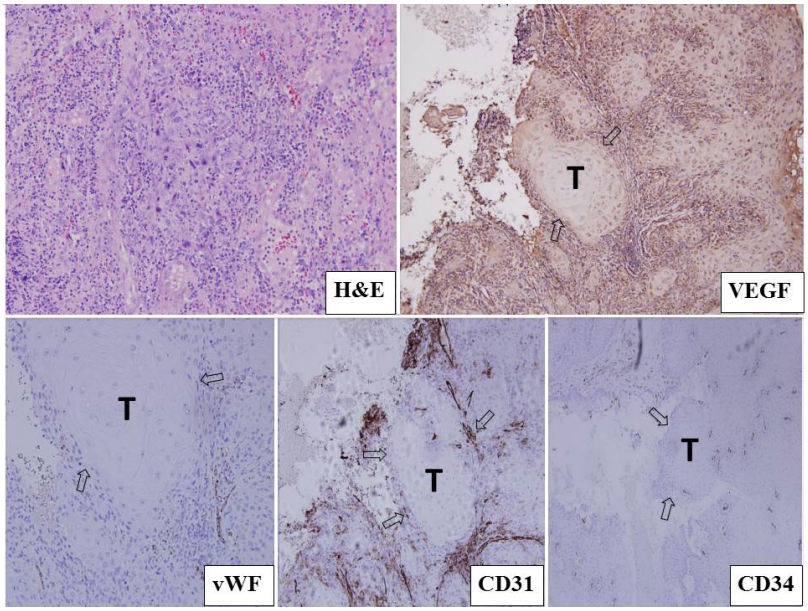


Fig. 4. H&E and immunohistochemical staining, including VEGF, vWF, CD31, CD34, of oral squamous cell carcinoma. Endothelial cell-lined blood vessels (arrows) were stained positive for VEGF, vWF, CD31, and CD34. There was a decrease of vessel staining around the tumor nest as compared to the granulomatous tissue in the stromal tissue layer of verrucous hyperplasia shown in Fig. 3. Symbol T represents tumor nest.

### *3.3 Compared to the controls, DRS detected higher $StO_2$ in SCC and VH lesions, and showed no difference in HK lesions*

Figure 5 plots the average $StO_2$ results from the buccal mucosa of normal subjects (i.e., the controls) and from the lesion sites (Fig. 5(A)) and adjacent tissue sites (Fig. 5(B)) of SCC, VH, and HK patients. Both lesion and adjacent tissue sites of SCC and VH patients showed well-oxygenated average $StO_2$ values that were either statistically (p-value $< 0.002$) or marginally (p-value $= 0.05$) higher than the controls. HK patients showed no different $StO_2$ from the controls (p-value $> 0.2$). Figure 5(C) depicts the $StO_2$ distribution from all subjects. Most SCC and VH lesions and their adjacent tissues were found to have $StO_2$ greater than 95% and most of the controls to have $StO_2$ less than 95%. The well-oxygenated SCC and VH lesions most likely came from the dense vasculature of granuloma and neovascular formation that are shown in Figs. 3 and 4. However, these DRS detected well-oxygenated results were not associated with the positive expression of HIF-1α shown in Table 1.

The ratio ($rStO_2$) of $StO_2$ in the lesion site over the adjacent tissue site was calculated for each patient and then averaged (Table 1). Figure 5(D) depicts the $rStO_2$ distribution. Several SCC patients showed $rStO_2$ values less than one, indicating relative hypoxia on the lesion sites compared to the surrounding tissue. This phenomenon was not observed in all VH and most of HK patients.

#195513 - $15.00 USD Received 12 Aug 2013; revised 17 Oct 2013; accepted 22 Oct 2013; published 29 Oct 2013

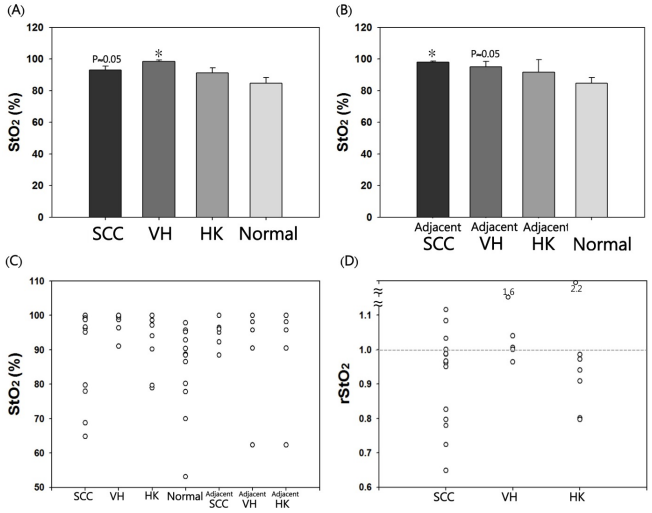


Fig. 5. Bar plots of average tissue blood oxygen saturation ($StO_2$) in lesion (A) and adjacent (B) tissue sites for squamous cell carcinoma (SCC), verrucous hyperplasia (VH), and hyperkeratosis/parakeratosis (HK) patients. Symbol * indicates the average $StO_2$ value is significantly different from the value of normal subjects, with a p-value less than 0.05. The distribution of $StO_2$ (C) and the $StO_2$ ratio ($rStO_2$) (D) for all patients. Each data point represents a single patient.

### *3.4 Differentiation between Verrucous Hyperplasia and SCC patients*

During conventional visual examinations in the clinics, HK appeared as a white plaque, but SCC and VH were not differentiable due to their similar appearance and color. As shown in Figs. 2 and 5, we have observed two unique features (i.e., higher blood volume and lower oxygenation in SCC lesions than the surrounding tissues) that DRS measurements provide to possibly differentiate between SCC and VH lesions, but not between SCC and HK or between VH and HK. We therefore tested the following criteria to see if SCC could be differentiated from VH patients. Figure 6 shows that we first applied an $rStO_2$ threshold value, $rStO_{2\_threshold}$, equal to 1.0 that separated 10 hypoxic SCC lesions from 10 of 11 VH lesions as shown in the left panel of Fig. 6. Then for those having $rStO_2 \geqq 1.0$, we applied another threshold value, $rTHC_{\_threshold}$, equal to 2.0 that separated 6 angiogenic SCC lesions from all of the 10 VH lesions as shown in the right panel of Fig. 6. Based on these two criteria, we calculated the sensitivity, or specificity, and accuracy to be 91%, 68%, and 76%, respectively.

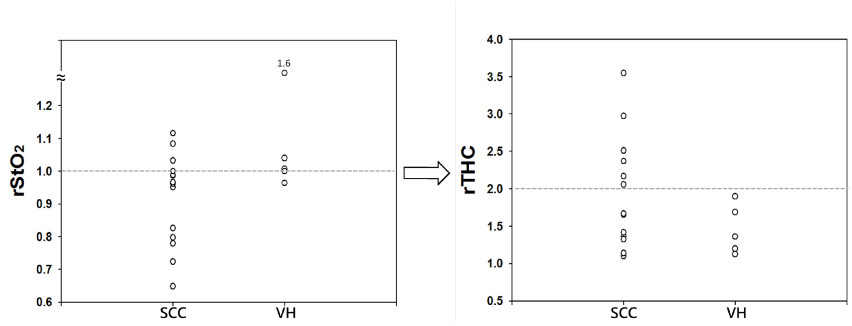


Fig. 6. Strategies to differentiate between squamous cell carcinoma (SCC) and verrucous hyperplasia (VH) patients by setting a threshold value of $rStO_2$ equal to one, and then rTHC equal to two, respectively. The relative hypoxia and angiogenesis features of SCC lesion compared to its surrounding tissue help differentiate SCC from VH, with a sensitivity greater than 90%.

#195513 - $15.00 USD Received 12 Aug 2013; revised 17 Oct 2013; accepted 22 Oct 2013; published 29 Oct 2013

**Table 2. Comparison of physiological properties measured from the human oral cavity *in vivo***

| *Technique* | *Reference* | *λ (nm)* | *detection depth (μm)* | *normal (mean± SE)* | | | *lesion (mean ± SE)* | | |
|---|---|---|---|---|---|---|---|---|---|
| | | | | **$n_{patient}$, $n_{site}$** | **THC (μM)** | **$StO_2$ (%)** | **$n_{patient}$, $n_{site}$** | **THC (μM)** | **$StO_2$ (%)** |
| **DRS** | this paper | 600-800 | 250-750 | 12, 120 | 130±10 | 85±4 | 22, 66 | 180±15 | 93 ± 2 |
| **DPS** | [7] | 350-1000 | ≤ 350 | 30[a] | 91±15 | 95±1 | 26[b] | 200±41[e] | 81 ± 4[e] |
| **DPS** | [8] | 350-1000 | ≤ 700 | 24[a] | 327± 54 | 94±1 | 15[c]& 12[d] | 191±49[c], 373±81[d,e,f] | 90±2[c], 89±4[d,e] |
| **DRS** | [30] | 380-700 | ≤ 250 | 88&99[g] | 73±9[f,g] | 60±1[g] | N/A | N/A | N/A |
| **DRS** | [31] | 520-820 | 533-800 | 2,6[h] | ~91-227[f,h] | ~70-75[h] | 2,10 | ~127-227[f] | ~60-75 |

[a] Normal subjects were measured as normal tissue; only number of subjects is listed.
[b] SCC was measured; only number of subjects is listed.
[c] Non-dysplastic leukoplakia was measured; only number of non-dysplastic patients is listed, as well as corresponding average THC and $StO_2$.
[d] Dysplastic leukoplakia was measured; only number of dysplastic patients is listed, as well as corresponding average THC and $StO_2$.
[e] Reported standard deviations (SD) were converted to standard error (SE = SD/√n). corresponding average THC and $StO_2$.
[f] Reported blood volume fractions were converted to hemoglobin concentration by multiplying by 150 (mg/ml); 1 mg/ml is approximately equal to 60.61 μM.
[g] The number of subjects for the average THC and $StO_2$ is 88 and 99, respectively. Only reported values for buccal mucosa from Table 2 are listed here. For multiple sites in the oral cavity, THC was reported to have a range of 12-170 μM (0.4-2.8 mg/ml), and $StO_2$ has a range of 60 and 70%.
[d] Periphery tissue of lesions was measured.

## 4. Discussion

In this study, we quantified THC and $StO_2$ in SCC, VH, and HK lesions and their adjacent tissues from 40 patients, as well as in the buccal mucosa of 12 normal subjects, using DRS. Table 2 shows the comparison of our results and other published works in quantifying oral normal and lesion tissues *in vivo* using optical spectroscopy. The wavelength range used and the estimated depth from tissue surface are listed as well. From the results of normal tissues and/or normal subjects, two studies from Amelink et al. [7, 8] show that THC tripled in value when the measurement depth doubled from 350 to 700 μm. Our penetration depth is estimated to be between 250 to 700 μm, and our measured average THC value of normal subjects fell between the results of these 2 studies. Our measured average THC value is higher than that by McGee et al., probably due to the detection depth used. McGee et al. [30] used shallower detection depth (less than 250 μm) than ours, so that study probably collected values only from the epithelial layer, without including values from the stromal layer. In terms of $StO_2$ measurement, our values from normal subjects were lower than those found by Amelink et al. but higher than those found by McGee et al. Rohrbach et al. [31] reported both THC and $StO_2$ values of two oral lesions and their corresponding periphery tissue. Our THC values of lesions are similar to theirs with higher $StO_2$ values. The discrepancy in $StO_2$ between different studies is likely due to various causes, including technology used (DRS *versus* DPS), the volume and depth detected, and different subjects or populations.

We detected higher THC in SCC than normal subjects, but did not detect higher THC in SCC than in VH and HK. One main reason is that inflammation-induced neovascular formation in VH and HK was also detected by optical spectroscopy. The incapability of separating inflammation-induced-neovasculature from angiogenesis-induced-vasculature using optical spectroscopy may hinder the accuracy of using optical spectroscopy in detecting tissue angiogenesis. As stated earlier, controversial results were reported for the relationship of angiogenesis and tumor malignancy, metastasis, and prognosis in oral cancer. However, by carefully examining inflammation-free areas, Gandolfo et al. were able to demonstrate a good

#195513 - $15.00 USD Received 12 Aug 2013; revised 17 Oct 2013; accepted 22 Oct 2013; published 29 Oct 2013

correlation of epithelial VEGF and sub-basal vascularization with malignancy in oral mucosa [27]. Therefore, optical spectroscopy should be used carefully when intended to only detect angiogenesis induced vascular formation for differentiating the degree of malignancy.

The similar inflammation-induced neovascular formation was possibly attributed to the significant higher THC in the adjacent tissues (within 1 cm from the lesion boundary) of VH lesions than normal subjects as shown in Fig. 2(B). Further study will be required to perform more DRS spatial distribution measurements and acquire biopsy in these adjacent sites to confirm their correlation.

An interesting finding of this study is the different ratio of $StO_2$ and THC levels between lesions and the adjacent tissues among lesions. Relative higher THC and lower $StO_2$ in lesions compared to the surrounding tissues were detected in majority of SCC patients but not in VH and HK patients. By applying such characteristics, SCC was differentiated from VH with a sensitivity of 91%. At present, SCC is not differentiable from VH by visual examination in the clinics. Further study with a larger number of patients would be necessary to confirm the findings of this study.

Similar to other reported studies [32], our immunohistochemical stains showed that VEGF and vascularity were not correlated. We observed higher blood vessel distribution in stromal layer than epithelial layer in HK and VH lesions, and found abundant microvessels around tumor nests in SCC lesions based on three blood vessel markers (vWF, CD31, and CD34). As with other published studies, these newly-formed capillaries in tumors have fragmented basement membranes and are leaky [33]. However, VEGF expression appeared evenly almost everywhere, showing no difference between epithelial and stromal layer in HK and VH. VEGF was slightly less expressed in the tumor nest of SCC compared to the surrounding stromal tissues (Table 1). In fact, vascularity rather than angiogenic factor expression has been used as an alternative and more direct index of angiogenesis [34] through markers like CD34 and CD31, which react with not only "newly formed" vessels but also normal vessels recently trapped within tumor tissue [35].

It is now believed that the pattern of angiogenesis may play a more important role in tumor invasion and metastasis [34] than the volume of neo-vessel formation. Kademani et al. [36] found that a penetrating pattern of neovascularity was associated with a statistically significant risk of cervical lymph node metastasis when compared with a circumscribing pattern. Zätterström et al. found low median survival (10 months) in tumors with very low microvessel density, compared to tumors with high microvessel density (69 months) [37]. Thus, the decrease of peri-tumor nest microvessels observed in SCC in our study may indicate greater tumor penetration and invasion capability, and may imply poor prognosis and possible metastasis.

Our $StO_2$ measurements show well-oxygenated status in most lesions (Fig. 5). This result is not correlated with our HIF-1α staining, where positive and even expression was shown in all lesions (Table 1). The similar positive and even expression pattern was seen in the VEGF staining of this study. Studies have shown that HIF-1α was correlated with VEGF [38], but was not correlated with tissue oxygen partial pressure ($pO_2$). HIF-1α, glucose transporter-1, and carbonic anhydrase, which are considered to be suitable as surrogate biomarkers of hypoxia, have been found to have no correlation with tissue $pO_2$ in cervical cancer patients [38–40]. Mayer A et al. even suggested that the term endogenous hypoxia markers should be avoided at least in the clinical oncology setting [40]. A study by Bearsley NJ, et al. has found that positive HIF-1α expression is associated with better survival for patients after surgery. They suggested that caution should be exercised because the specificity of interactions with HIF system, the specificity to areas of tumor rather than physiological hypoxia, and the overall effect of inhibiting the HIF system are unclear [41]. In our histologic study, high vessel density was found in the inflammatory lesion's stromal areas, especially in VH, which showed a higher percentage of granulomatous/inflammatory response below the epithelial layer. Our results suggest that DRS measured well oxygenation in most lesions and their surrounding tissue are in part due to inflammation induced blood vessel growth.

#195513 - $15.00 USD Received 12 Aug 2013; revised 17 Oct 2013; accepted 22 Oct 2013; published 29 Oct 2013

In summary, we performed DRS to quantify tissue THC and $StO_2$ in the buccal mucosa of normal subjects as the controls, and in the lesion and adjacent tissue sites of SCC, VH, and HK patients. We compared these quantified physiology findings with multiple immunohistochemistry stains, including Hif-1α for hypoxia and VEGF, CD31, CD34, and vWF for angiogenesis and blood vessel volume. We found higher THC and $StO_2$ in most of lesions and their adjacent tissue compared to the controls. Our immunohistochemistry results also showed high blood vessel volume in all lesion specimens due to neovascular formation induced by angiogenesis and/or granulomatous/inflammatory response. Higher THC and lower $StO_2$ were detected by DRS in SCC lesions compared to their surrounding tissues, but not in VH or HK. These two features allowed the differentiation between VH and SCC with a sensitivity of 91%. This result suggested that DRS detected relative THC and $StO_2$ between lesions and surrounding tissue may be potential screening parameters in aiding oral cancer screening or diagnosis. Further understanding the nature of the spatial distribution of such relative angiogenesis and hypoxia features in SCC lesions is under investigation in our research group.

**Acknowledgments**

This work was supported by the "Aim for Top University Plan" from the Ministry of Education of Taiwan, and by grants NSC98-2112-M-010-003-MY3 from the National Science Council of Taiwan and TCVGH-995602C from Taichung Veterans General Hospital.

#195513 - $15.00 USD Received 12 Aug 2013; revised 17 Oct 2013; accepted 22 Oct 2013; published 29 Oct 2013